Structure and potential applications of polyamide 6/protein electro-spun nanofibrous mats in sorption of metal ions and dyes from industrial effluents

Salwa Mowafi[a] • Marwa Abou Taleb[a] • Claudia Vineis[b] • Hosam El-Sayed[a]*

[a]Textile Industries Research Division, National Research Centre, Giza, Egypt
[b]CNR-STIIMA, National Research Council-Institute of Intelligent Industrial Technologies and Systems for Advanced Manufacturing, Italy

Abstract: The main objective of this work is the preparation of nanofibrous mats (NFM) from polyamide 6 (PA6) reinforced and functionalized by renewable proteinic waste and examining their potential use for the sorption of heavy metal ions and dyes from wastewater from textile plants. Two renewable waste biopolymers; namely keratin (from waste of wool combing) and sericin (from degumming of natural silk) were extracted and regenerated. NFMs were prepared by electro-spinning of PA6/biopolymer composites in formic acid using nozzle-less electro-spinneret. The potential of the prepared mats for sorption of Cr^{+6}, Cr^{+3}, Cu^{+2}, and Pb^{+2} cations as well as anionic and cationic dyes from wastewater were assessed. The prepared composites were characterized by measuring their viscosity, nanofiber diameter, porosity, thickness, and air permeability. The morphological structure of the electro-spun NFM was investigated by scanning electron microscopy (SEM). Chemical and physical properties of the obtained mat were studied using Fourier Transform Infrared Spectroscopy (FTIR), thermal gravimetric analysis (TGA), differential scanning calorimetry (DSC), and X-ray diffraction pattern (XRD).

In the NFMs from PA 6 only, PA 6/keratin, PA 6/sericin, and PA 6/keratin and sericin, the sorption capacity of the prepared NFMs towards the examined cations varies according to the NFM composition and the nature of the adsorbed cation. In all cases, the maximum dye sorption was attained after 96 hours for basic dye and 72 hours for acid dye.

---

*Corresponding author.
E-mail address: hosam@trdegypt.org (Hosam El-Sayed).

1. Introduction

There are many areas growing and imposing excessive demands on water, resulting in a much-expected exhaustion of water and its resources. Industrial developments resulted in accumulation of many pollutants; Viz. heavy metal ions (Pool, 2020), dyes (Alhujaily et al., 2020), and pharmaceutical wastes (Abdel-Gawad & Abd El-Aziz, 2020) in water effluents. Humans contact with such toxic pollutants poses a major health risk because of their carcinogenic and toxic effects (Abdel-Halim et al., 2003). Some of the most toxic and carcinogenic heavy metal ions include Pb^{+2}, Cd^{+2}, As^{+3}, Cu^{+2}, Ni^{+2}, Cr^{+3}, and Cr^{+6} cations (Awual, 2015; Gautam et al., 2015; Lunge et al., 2014; Madadrang et al., 2012; Wang et al., 2014; Xu, et al., 2014). These heavy metals are not only causing pollution to water, but they are also life-threatening (Wang et al., 2014) such as causing damage to the central nervous system and kidneys in humans.

The regulations of the World Health Organization (WHO) based on the Environmental Protection Agency (EPA) amendments assigned the permissible limit for Pb^{+2} in wastewater at 0.05 mg/L (Goel et al., 2005; Ucun et al., 2003). To mitigate the lead ions pollution, many processes like adsorption, precipitation, coagulation, ion exchange, cementation, electro-dialysis, electro-winning, electro-coagulation and reverse osmosis have been developed (Al-Shannag et al., 2015). On the other hand, the WHO recommended safe limits for Cr^{+6} in wastewater is 0.05 ppm (Aneyo et al., 2016).

Dyes discharged from the dye lines for coloration of textiles are considered as other threatening pollutants within the textile effluent. Because of the serious risks that pose to humans, dye removal is an extremely important issue to deal with. Carcinogenic effects have also been observed in a few dyes, and their degraded products are present in surface water (Kannan & Sundaram, 2001). Hence, it is important to clean or to pre-treat these dye effluents before discharging them into water resources.

There are many scientific methods and materials that have been proposed and tested for water desalination and purification. Among those materials, nanomaterials in the form of nanoparticles or nanofibers with different morphologies have potential impacts for treating water, and have been observed to be very effective in removing heavy metal ions, toxic metals, dye, and other harmful organic solvents (Nasreen et al., 2019). Nanofibrous membranes are commonly studied materials for water filteration applications (Balamurugan et al., 2011; Gopal et al., 2007). Many polymeric nanofibers that are fabricated by the electro-spinning method have been shown to exhibit unique filtration properties (He et al., 2014; El-Sherif et al., 2013; Karthi & Meenakshi, 2015; Liu et al., 2013; Mahapatra et al., 2013; Rad et al., 2014; Sounthararajah

et al., 2015; Xu et al., 2014; Zhao et al., 2015; Zhou et al., 2011). Other reported technologies for heavy metal ions removal include utilization of activated carbon (Bohli et al., 2015), clay (Gu et al., 2019), and nanosized metal oxides (Hua et al., 2012). However, most of these technologies are relatively expensive and use high-cost materials.

Biopolymers are macromolecules fully or partially produced in a natural way by living organisms. Because of their biodegradability into carbon dioxide and water (Moore, 2008), biopolymers are now significant for many fields including food technology, nanotechnology, chemistry, textile, medicine, agriculture etc. According to market research, consumers are willing to pay more for bio-based polymers, and their market shows huge growth; reached to 3 million tons per year by 2013 and 7 million tons by 2018 (Carus et al., 2013). Keratin and sericin are considered to be proteinic biopolymers that emitted to the environment as by-products. Several research papers have dealt on the extraction and recovering of these biopolymers from their natural resources for further utilization in several fields (AbouTaleb et al., 2020; El-Newashy et al., 2019; Mowafi et al., 2018).

This work aims at preparation of nanofibrous mats based on polyamide 6 together with renewable benign biopolymer wastes, namely keratin and sericin. The prepared electro-spun nanofibrous mats are utilized in sorption of heavy metal ions and dyes from effluents of textile plants. This work meets some environmental and economic demand by extraction of keratin and sericin from waste materials and their utilization in reinforcement of PA6 NFM for sorption of selected cations as well as dyes from textile effluents.

2. Materials and methods

2.1. Materials
Natural silk fibers were kindly provided by the Sericulture Department at the Agricultural Research Centre, Ministry of Agriculture and Land Reclamation. Waste of combing of wool fleece was collected from small enterprises. Wastes of polyamide 6 (PA6) fibers of average molar mass 22500 g/mole were provided by MisrBeida Dyers, Egypt. Formic acid (98%) was purchased from Sigma Aldrich. sulphuric acid, acetic acid, sodium carbonate, and ammonium chloride were purchased from ADWIC, Egypt.

2.2. Methods
2.2.1. Scouring
Wool fleece was scoured in an aqueous solution containing 1g/L Na_2CO_3 at 50°C for 30 min with M:L ratio 1:50. The scoured wool fleece was rinsed thoroughly with tap water and air-dried at ambient temperature.

2.2.2. Extraction of keratin

Keratin was extracted from their scoured wool fleece by dissolution in an aqueous solution of 0.2M sodium hydroxide at 70 °C for 30 min. A 200 mL coagulating bath was prepared for precipitation of 100 mL soluble keratin solution. This bath is an aqueous solution containing 12% NH_4Cl and 6% H_2SO_4 (w/v). The regenerated keratin was well-rinsed with distilled water till pH 7 and left to dry overnight then ground into powder form.

2.2.3. Degumming of sericin

Raw natural silk sample was dipped in boiling water through three consecutive cycles; 1 h each (water was refreshed in each cycle). Sericin was precipitated from the degumming effluent by adjusting the pH around the isoelectric point of sericin (*ca.* 4). The precipitate was filtered to collect sericin and left to dry at ambient temperature, and then pulverized in a mortar.

2.2.4. Preparation of electro-spun composite

A 25 % (w/v) solution was prepared by dissolving 20 % PA 6 fibers together with 5% regenerated keratin, sericin, or mixture thereof in concentrated formic acid (98%). The composites of PA 6/keratin (PA 6/K), PA 6/sericin (PA 6/S) and PA 6/keratin/sericin (PA6/K-S) were mixed together with magnetic stirrer (500 rpm) for about 15 min at room temperature (*ca.* 25 °C) till complete dissolution.

It is noteworthy to mention that different concentrations and ratios of PA 6, sericin, and keratin were adopted to obtain electro-spinnable composite material of appropriate viscosity. Based on many viscosity measurements and electro-spinning trials, we found that the most appropriate concentrations and ratios of PA 6 and the said biopolymers are those mentioned above.

2.2.5. Preparation of the nanofibrous mats

The prepared biopolymer-based composites (about 10 mL each) were electro-spun into nanofibrous mats using ELMARCO nozzle-less Electro-spinneret (Liberec, Czech Republic). The applied electric potential was 30–35 kV. The collector was mounted at 13 cm away from the wire and the solution carriage speed was kept at 100 mm/s, which was found to be the appropriate speed for creation of nanofibers. The process of nozzle-less electro-spinning was conducted for about 45–60 min at 22°C and 65% relative humidity.

2.2.6. Preparation of heavy metal solutions

Four stock solutions of 0.04 mmole/L of potassium dichromate [$K_2Cr_2O_7$], chromium III chloride hexahydrate [$CrCl_3.6H_2O$], copper II sulphatepentahydrate [$CuSO_4.5H_2O$], and lead acetate [$(CH_3COO)_2Pb$] were prepared for synthetic wastewater during this investigation. In all solutions, the pH of the prepared said solutions was not modified and used as it is. Alkaline pH values were prohibited as it will cause precipitation of each cation from its solutions (Sum et al., 2019).

2.3. Analyses and testing

2.3.1. Scanning electron microscopy

The surface morphology as well as the fiber diameter of the prepared nanofibrous mats was examined by ZEISS LEO 1530 Gemini Optics Lens Scanning Electron Microscope (SEM) with 30 kV scanning voltage. The samples were mounted on aluminum stubs, and sputter coated with gold in an S150A sputter (coated Edward, UK). The nanofibers' diameters were measured from the scanning electron micrographs and the porosity of each sample was also determined using Image J software (Haeri & Haeir, 2015).

2.3.2. Viscosity measurement

The viscosity of the prepared composites was measured at 10 rpm using Programmable Rheometer (Model DV III), Brookfield Engineering Labs, MA, U.S.A.

2.3.3. Batch sorption investigation

The sorption aptitude of the prepared chelating nanofibrous mats for Cr^{+6}, Cr^{+3}, Cu^{+2}, and Pb^{+2} cations was monitored by the batch method and single element system for different contact period of times. Dried sample of 0.1 g of each prepared mat was added in 100 mL Erlenmeyer flask containing 50 mL of each of the said cation solution. The mixture was maintained at 25 °C with gentle agitation for 2, 10, 24, 48, 72, and 96 hours. The solution was filtered and the metal ion concentration was measured using a Perkin Elmer Analyst 4100 ZL atomic absorption spectrometer.

2.3.4. Dye adsorption

A 0.05 g of the prepared nanofibrous mats was immersed in a 50 mL of 20 ppm methylene blue dye of pH 6 at room temperature. A sample of the dye was taken after different periods of time 2, 24, 48, 72 and 96 h. The absorbance was measured on a UV-spectrophotometer to determine the dye exhaustion by the mats at λ_{max} 665 nm.

In another experiment, the prepared mat was immersed in a sample from an industrial dye effluent (pH 1.8) containing an acid dye. A 0.05 g of the prepared nanofiber mat was immersed in 50 mL of the said dye-containing effluent. The absorbance of the dye is measured after 2, 24, 48, 72, 96 h to at λ_{max} 505 nm.

2.3.5. Fourier transform infrared spectroscopy

Infrared spectroscopy was carried out for the prepared mats of biopolymer and PA6 on Fourier transform infrared spectrometer (JASCO FTIR-4700, Japan) in the region of 4000–400 cm^{-1} with spectra resolution of 4.0 cm-1.

2.3.6. Thermal properties

Thermal gravimetric analysis (TGA) and differential scanning calorimetry (DSC) were measured using SDT Q2000 Tzero DSC from TA instruments under nitrogen atmosphere with a rate of heating 10 °C/min.

2.3.7. X-ray diffraction pattern

The X-ray diffraction pattern was assessed on a Bruker D8 Avance using Cu Kα as the target with secondary mono-chromator to operate at 40 KV and 40 mA. The scans were performed within the range of 4° < 2θ < 60° with scanning step 0.02° in reflection geometry. The crystallinity index (CI) was calculated using the following empirical Eq.1:

$$CI = [(I_c - I_a) / I_c] \times 100 \tag{1}$$

where, CI is the crystallinity index; I_c is the maximum intensity of crystal lattice diffraction and I_a is the minimum diffraction intensity. In general, higher CI value indicates higher crystallinity of the nanofiber sample.

2.3.8. Air permeability

Air permeability of the prepared mats was examined according to ASTM D737 standard method on an FX 3300 air permeability tester (TEXTEST AG, Switzerland) at a pressure of 100 Pa. The measurement was carried out with a 1.4 mm orifice, 17.7 cm^2 test area, at 762 mm mercury pressure, 20°C, and 65% relative humidity (Vitchuli et al., 2011).

3. Results and discussion

3.1. Nanofiber morphology and properties

Figure 1(a–d) shows the SEM micrographs of nanofibrous mats (NFM) obtained by electro-spinning PA6, PA6/K, PA6/S, and PA6/K-S composites, respectively. It easy to notice in this figure that the nanofibers obtained from each solution are haphazardly disseminated on the mats, creating a non-woven web. As declared in Table 1, the diameter of the obtained fibres lies within the nanorange which provides huge surface area of the prepared mats and consequently one would expect a high capacity of capture of metal ions and dyes from effluents.

Data in Table 1 elucidates that the thickness, diameter, air permeability, and porosity of the prepared NFM mats increased in the order: PA6<PA6/S< PA6/K-S<PA6/K. The high porosity of PA6/K NFM makes it effective as a membrane for effective filtration. It has been reported that effective filters are characterized by their high porosity, interconnected open pore structure, high permeability, and a large surface area per unit volume (El-Sayed et al., 2019; Gopal et al., 2006; Tsai et al., 2002).

The hydrophobic nature of PA6 NFM would account for the relatively small fibre diameter the nano-fibres obtained by electro-spinning of this polymer from its solution (Dhineshbabu et al.,2014), whereas the maximum fibre diameter obtained from electro-spinning of PA6/K composite is due to its low viscosity relative to the other solutions used in this investigation (Nezarati et al., 2013). Other factors that may affect the electrospun fibre diameter include the applied voltage, the used polymer concentration, the nature of solvent, and the polymer flow rate (Haidar, et al., 2018; Mit-ippatham et al., 2004).

Results shown in this table reveal also that PA6/K NFM is the most air-permeable sample. Although this sample has greatest thickness (0.16 mm) than the other samples, yet it also has the largest pore size (3715 ± 10 nm) which rationalizes the highest air permeability. Aizawa and Wakui reported that gas permeability is a function of nanofibers porosity in a direct relationship (Aizawa & Wakui, 2020).

3.2. Metal adsorption

Removal of heavy metal ions, which are usually used in textile industries, from their effluents is of prime importance from the ecological point of view (Tetteh & Rathilal, 2020; El-Sayed et al., 2004). Table 2 summarizes the results of the efficiency of different PA6/biopolymer-based NFM in removing some heavy metal cations from their solutions for different period of times. Scrupulous investigation of this table infers the following:

The efficiency of PA6 NFM for adsorption of metal ions from their solution is in the order: $Cr^{+6} > Pb^{+2} > Cr^{+3} > Cu^{+2}$. At pH 5, Cr (VI) exists in the aqueous solution of $K_2Cr_2O_7$ in a form of hydrogen chromate ion ($HCrO_4^-$), this would increase the interaction of the positively charged protonated amino groups in PA6 and the formed negatively charged species; and hence facilitates chelation of Cr VI ion with the amino groups of PA6 (Chen et al., 2008; Minif et al., 2017). The relatively high affinity of PA6 towards Pb^{+2} ion may be attributed to the relatively low hydrated ionic radius of Pb^{+2} (401 pm) which enables it to diffuse easily into the fiber interior followed by chelation of the metal ion by the lone pair of electrons of the nitrogen atom of the amino groups in PA 6 (Mobashepor et al., 2012). The relatively large radii of the hydrated Cr^{+3} and Cu^{+2} ions (461 and 419 pm, respectively) would account for the lower efficiency of PA6 to adsorb these cations from their solutions. A more significant reason that would hindered the absorption of Cu^{+2} and Cr^{+3} ions onto PA6 is the relatively strong acidic media of the respective used salts (pH 3.5–4.0 for the former and 2.0–3.0 for the latter). There will be strong repulsion force between these cations and the protonated amino groups in PA6 macromolecules, consequently the chelation of these cations will be hindered.

Similar trends were observed upon using PA6/K, PA6/S, and PA6/K-S NFM for removal of the same cations from their aqueous solutions ($Cr^{+6} > Pb^{+2} > Cr^{+3} > Cu^{+2}$).

The order of the efficiency of the used NFM mats in sorption of Cr+6 ions from its aqueous solution is: PA6/S ≈ PA6/K-S > PA6/K > PA6. The superior sorption ability of PA 6/S may be attributed to the synergetic effect of the large number of chelating amino groups along sericin macromolecules. In case of PA6/K composite, instead of chelation of Cr^{+6} ion by the amino groups, a reversible redox reaction between Cr^{+6} ions and the thiol groups along keratin macromolecules was taken place (Chakraborty, 2014).

$$2W-SH + Cr^{+6} \rightleftharpoons W-S-S-W + Cr^{+3} \tag{2}$$
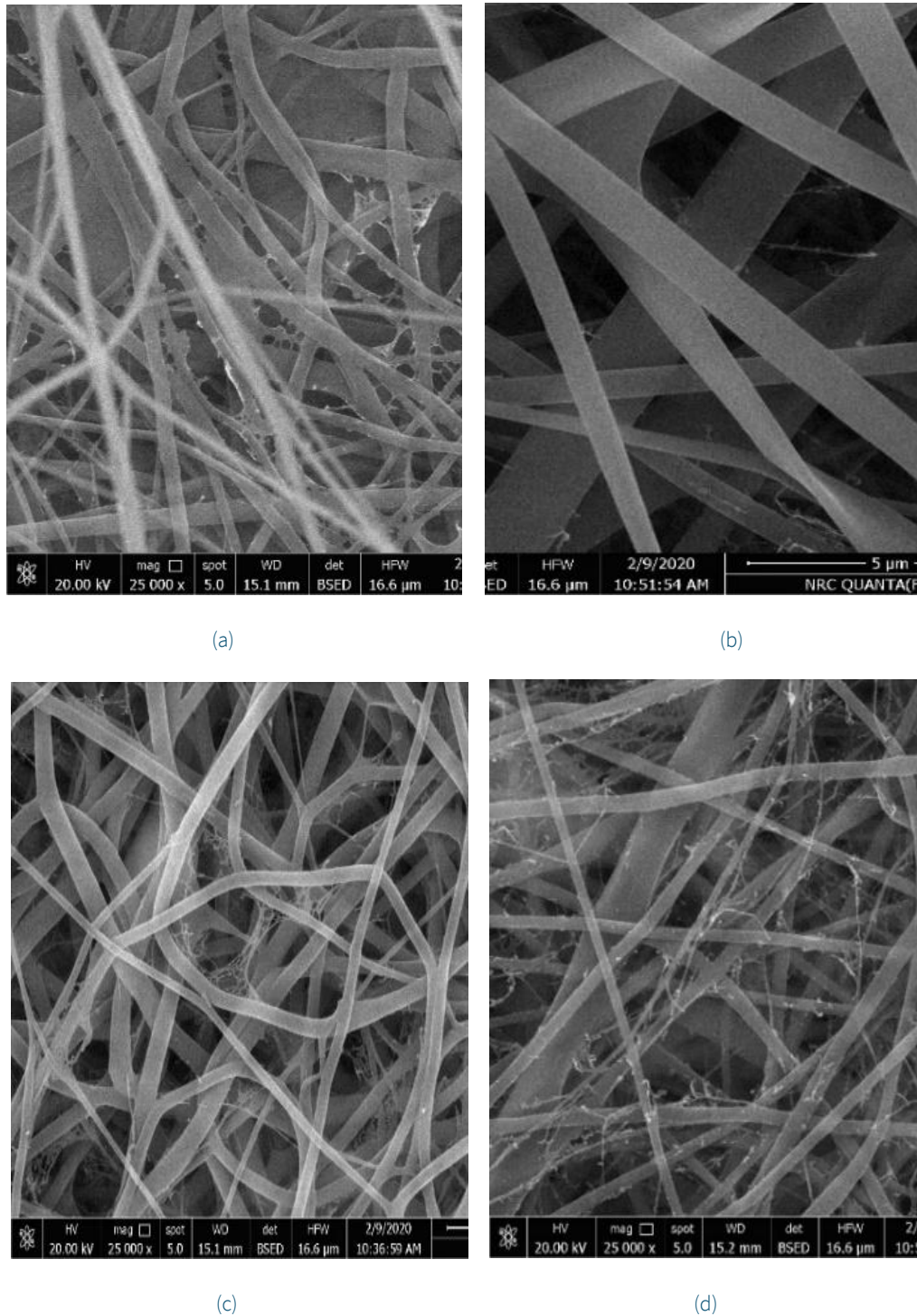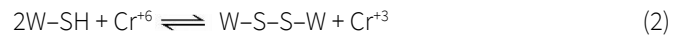

(a)

(b)

(c)

(d)

Figure 1. Scanning electron micrographs of electro-spun NFM prepared from solutions of (a) PA6, (b) PA6/K, (c) PA6/S, and (d) PA6/K-S composites.

Table 1. Viscosity of the PA6-based composites mats thickness, nanofiber diameter, pore size, and air permeability obtained by electrospinning of different PA6-based composites.

Sample	Viscosity (cp)	Thickness (mm)	Diameter (nm)[a]	Air perm. (cm³/cm².S)	Pore size (nm)		
					Minimum	Maximum	Mean
PA6 NFM	1000	0.06	150[b]	3.46	40	970	508.4±5
PA6/K NFM	4850	0.16	500[c]	4.49	430	7010	3715±10
PA6/S NFM	2000	0.09	200[d]	3.68	130	1990	1073±10
PA6/K-S NFM	4000	0.13	250[e]	3.61	200	4300	2250±10

a: average of 7 measurements of the diameter of 7 different nanofibres
b: Standard deviation is 1.29, c: Standard deviation is 2.04, d: Standard deviation is 1.34, e: Standard deviation is 2.01.

Table 2. Removal of some heavy metal ions from water using PA6/biopolymer NFM
(the initial concentration of the used heavy metal ions salts is 0.04 mmole/L).

NFM	Removal of metal ion (%) after																			
	2 h				24 h				48 h				72 h				96 h			
	Cr^{+6}	Cr^{+3}	Cu^{+2}	Pb^{+2}	Cr^{+6}	Cr^{+3}	Cu^{+2}	Pb^{+2}	Cr^{+6}	Cr^{+3}	Cu^{+2}	Pb^{+2}	Cr^{+6}	Cr^{+3}	Cu^{+2}	Pb^{+2}	Cr^{+6}	Cr^{+3}	Cu^{+2}	Pb^{+2}
PA6	17.0	6.3	1.2	15.0	37.0	7.3	2.5	16.6	46.9	8.4	8.86	17.5	53.9	9.5	12.6	71.7	52.6	12.6	16.4	84.1
PA6/K	25.3	7.4	5.1	30.0	37.1	10.5	21.5	34.2	56.9	12.6	29.1	56	60.7	15.8	32.9	81.7	51.4	16.8	32.9	89.0
PA6/S	30.2	4.2	6.3	8.3	50.0	5.3	8.86	10.0	64.3	7.4	12.6	13.3	64.3	10.5	17.7	13.3	63.3	13.7	16.5	16.0
PA6/K-S	33.6	6.3	8.8	15	45.7	10.5	12.6	16.6	64.2	12.6	13.9	20	64.3	13.7	18.9	23.3	63.5	17.9	17.7	26.6

On the other hand, sorption ability for removal of Pb^{+2} ions is in the order: PA6/K > PA6 > PA6/K/S > PA6/S. The relatively high sorption power of keratin-containing NFM might be explained in terms of the presence of additional chelating groups; namely, thiol groups along keratin macromolecule.

3.3. Dye adsorption

Sericin or keratin-containing NFM are suitable candidates for removal of anionic and cationic dyes by virtue of the cationic and anionic niches found along their polypeptide chains (AbouTaleb et al., 2019; Haggag et al., 2009; Kantouch et al., 2012). The said biopolymer composite with PA6 was adopted to remove methylene blue (cationic colorant) and an acid dye from a dye effluent (anionic dye). Cationic dyes are widely used in coloration of acrylic fabrics (El-Gabry et al., 2016) and the anionic dyes are the most commonly used class of dyes for coloration of proteinic fabrics (El-Sayed, 2006; Kantouch et al., 2011).

Figures 2 and 3 show that the sorption capacity of the regenerated PA6 NFM towards the used anionic dye is higher than the used cationic dye. This can be rationalized in terms of the protonated nitrogen-containing functional groups along the polyamide macromolecules. Results of Table III revealed also that the affinity of PA6/K, PA6/S, and PA6/K-S NFM towards the said dyes is higher than the corresponding PA6 samples, presumably, because of the synergetic effect of the polar functional groups in keratin and sericin in addition to PA6. In all cases, the máximum dye sorption is attained after 96 hours for basic dye and 72 hours for acid dye.

Generally speaking, the proposed NFMs may have comparable efficiency for removal of heavy metal ions as well as anionic and cationic dyes from wastewater, with other previously reported materials. Assuming that the prepared NFMs are better or worse than others from some or few points of views, however, the prepared NFMs have the advantage of being prepared from waste materials which makes the overall process cost-effective with positive ecological impact.
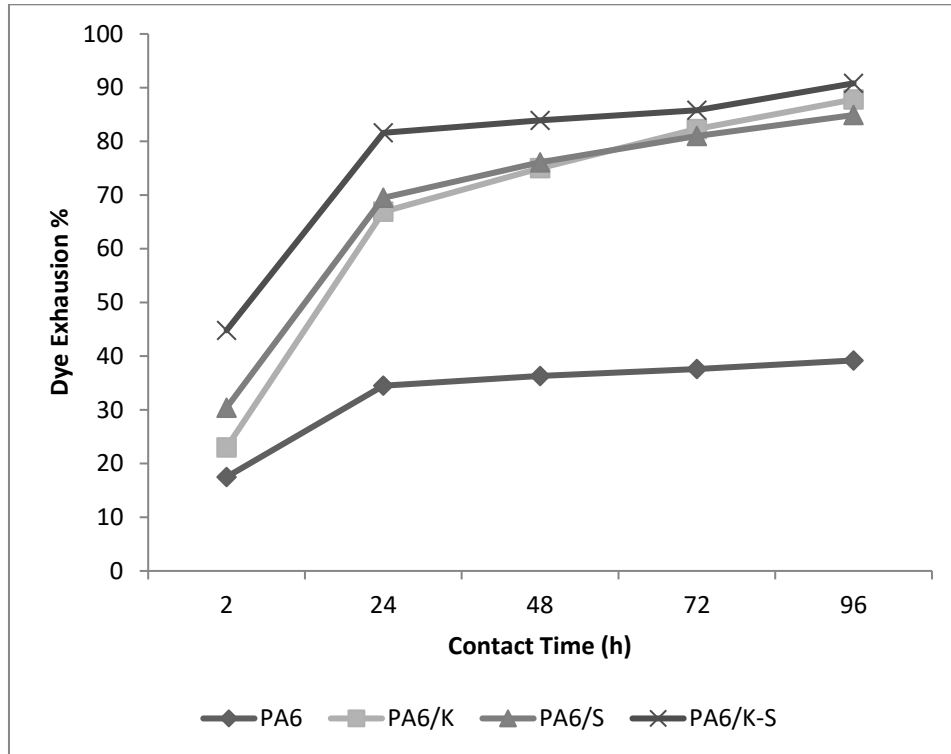
Figure 2. Exhaustion curve of anionic dye (an acid dye from dyehous effluent) PA6, PA6/K, PA6/S, PA6/K-S NFM.
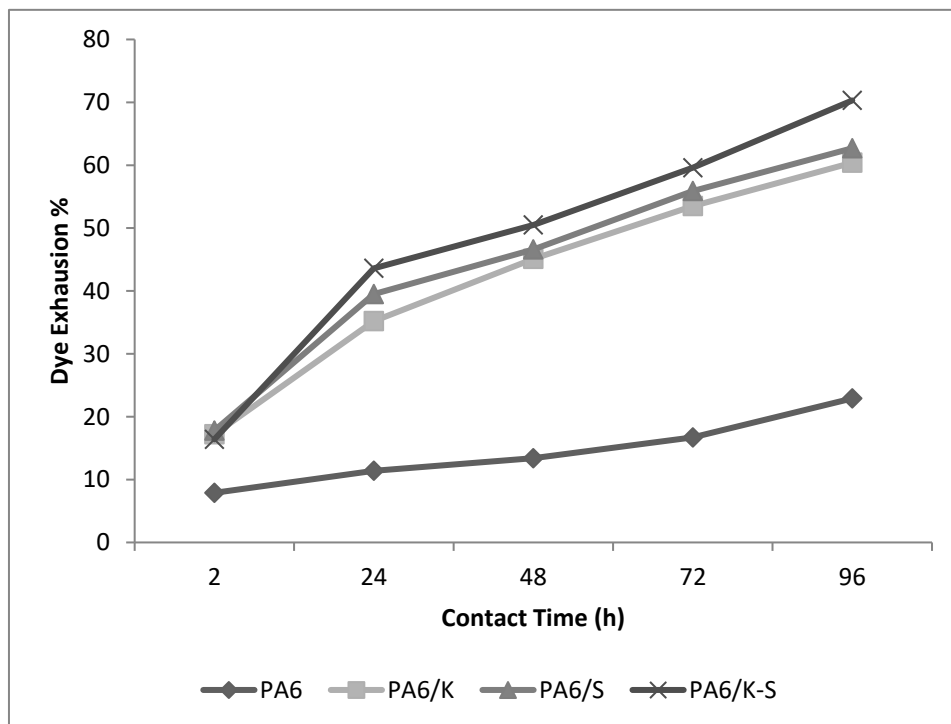

Figure 3. Exhaustion curve of cationic dye (methylene blue) by PA6, PA6/K, PA6/S, PA6/K-S NFM.

3.4. Fourier transform infrared spectroscopy

Figure 4 shows the FTIR chart of PA6 fiber, PA6 regenerated mat, keratin and sericin powder, PA6/K, PA6/S, and PA6/K-S NFM.

Spectra of polyamide 6 fibers as well as the corresponding regenerated electro-spun nanofibers show bands associated with the crystalline α form (1030, 960, 930 and 830 cm^{-1}) and the bands corresponding to amide V and amide VI in the α structure at 690 and 580 cm^{-1} respectively (Zoccola et al., 2007).

The FTIR spectrum of keratin displays characteristic band of amide I, amide II, and amide III at 1630 cm^{-1}, 1519 cm^{-1}, and 1235 cm^{-1} which belong to the stretching vibrations of the carbonyl group, the bending deformation of N–H bonds and stretching vibrations of C–N bonds, and C–N bond stretching and N–H in-plane bending vibrations (Cheng et al., 2016; Jose et al., 2019). Sericin has a broad amide A band at 3270 cm^{-1}, and amide I and II peaks at 1650 and 1530 cm^{-1} (Zhang & Wyeth, 2010).

Figure 4 elucidates also that the FTIR spectra of the NFM composed of PA6 and keratin, sericin, or mixture thereof comprise all the bands found in each substrate. Furthermore, no distinguishing new bands were observed in the said FTIR spectra. This implies that no alteration in the functional groups along both PA6 and protein macromolecules during formation of their composites. Consequently, the mode of action between PA6 and the said biopolymers is only physical interaction and not chemical bonding.

3.5. Thermal properties

The thermal behavior of the prepared NFM was monitored using differential scanning calorimetry (DSC) and thermal gravimetric analysis (TGA).

Figure 5 elucidates that the temperature at which maximum decomposition of the NFM was attained between 440–489°C depending on the mat composition. Among all tested samples, PA6 mat was almost entirely degraded at 445°C, while only 44.5 % of PA6/K-S mat was deteriorated at 450°C. Results of these tables reveal also that PA6 mat was utterly decomposed at 469°C. On the other hand, about PA6/K and PA6/S mat withstand heating until 490.5°C. About 11 % of the former and 5.5 % of the latter remained intact at such temperature. Maximum thermal stability was recorded for PA6/K-S which retains about 45% of its mass intact until 590°C. This result is a strong clue that sericin and keratin reinforce PA6 mats and lead to via formation of extra physical bonds; viz. hydrogen bond between the said macromolecules.

3.6. X-ray diffraction (XRD) pattern

Figure 6 and Table 3 summarize the main findings of the XRD pattern of PA6 fiber as well as its NFM with keratin and sericin. It was established that PA6 exhibits two main crystalline forms, namely α and γ. PA6 fiber has a sharp peak at 21.4° that corresponds to crystalline γ- form as dominant phase and two short shoulders at approximately 2θ= 20° and 23.7° for the α-crystalline form (Fornes & Paul, 2003). It can be seen from the data of Table III that, formation of the nanofibrous mats of PA6 leads to conversion of the α-structure of PA6 to γ-crystallineform. This hypothesis is supported by the appearance of 2θ at 21.8° and the decrease of the crystallinity from 43 to 33. The data in this table shows also that the characteristic peaks of keratin and sericin are present at 2θ, 10.0 and 11.7; respectively (ki et al., 2007; Liu et al., 2015).

As displayed in Table 3, the crystallinity of PA6/K, PA6/S, and PA6/K-S NFM is more than that of the analogous nativepolymers. This may be attributed to the formation of physical bonds; viz. hydrogen bonds, between the polar groups along PA6, keratin, and sericin macromolecules which decreases the freedom of the polymer chains and results in creations of more crystalline areas (El-Newashy et al., 2019).

Figure 6 shows that there are two peaks appeared in the XRD pattern of PA6/K sample at 2θ (21.8° and 6.8°), PA6/S sample (at 2θ 24.06° and 9.1°), and PA6/K-S sample (at 2θ 20.3° and 6.7°). The peaks at 2θ 21.8°, 24.06°, and 20.3° belong to PA6; whereas those at 2θ 6.8°, 9.1°, and 6.7° correspond to keratin, sericin and their blend, respectively. The discrepancy in the 2θ value of keratin and sericin in the PA6/K and PA6/S NFM relative to the corresponding native ones assures the binding of keratin and sericin into PA6 polymeric chains, also the shift in the d-spacing emphasizes this hypothesis.
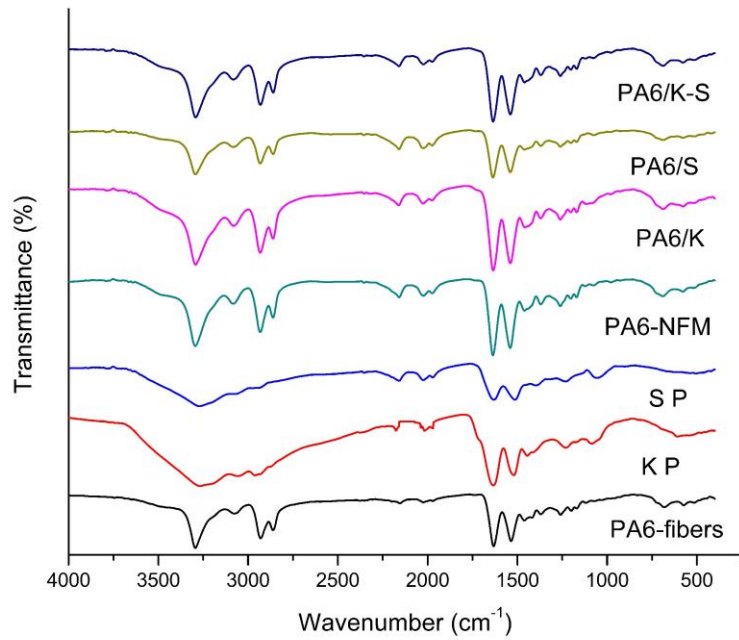
Figure 4. FTIR spectra of PA6 fibers, keratin powder (KP), sericin powder (SP), and the nanofibrous mats derived from them.
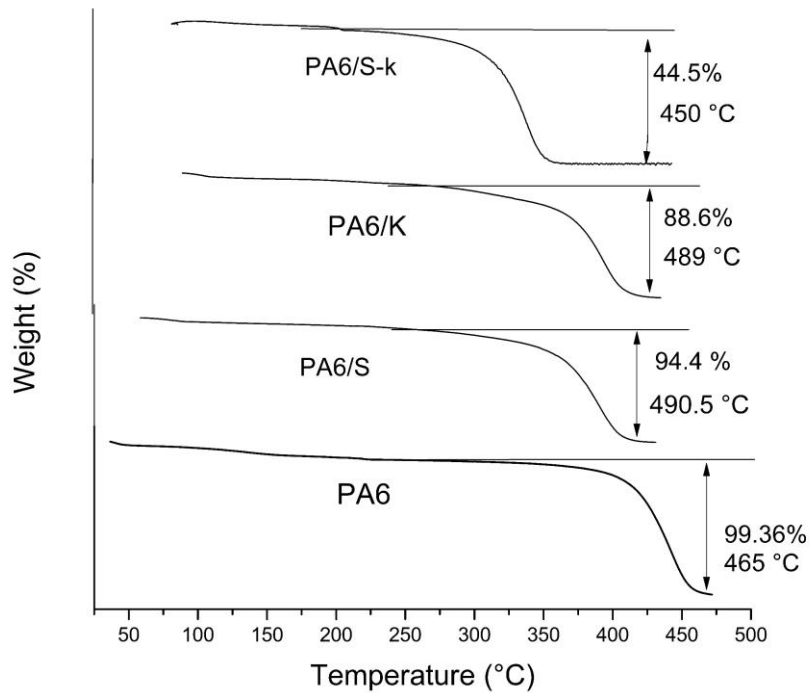

Figure 5. TGA curve of PA6, PA6/K, PA6/S, and PA6/K-S nanofibrous mats.

Table 3. Crystal structure of PA6 fibers, keratin, sericin,
and PA6-based nanofibrous mats.

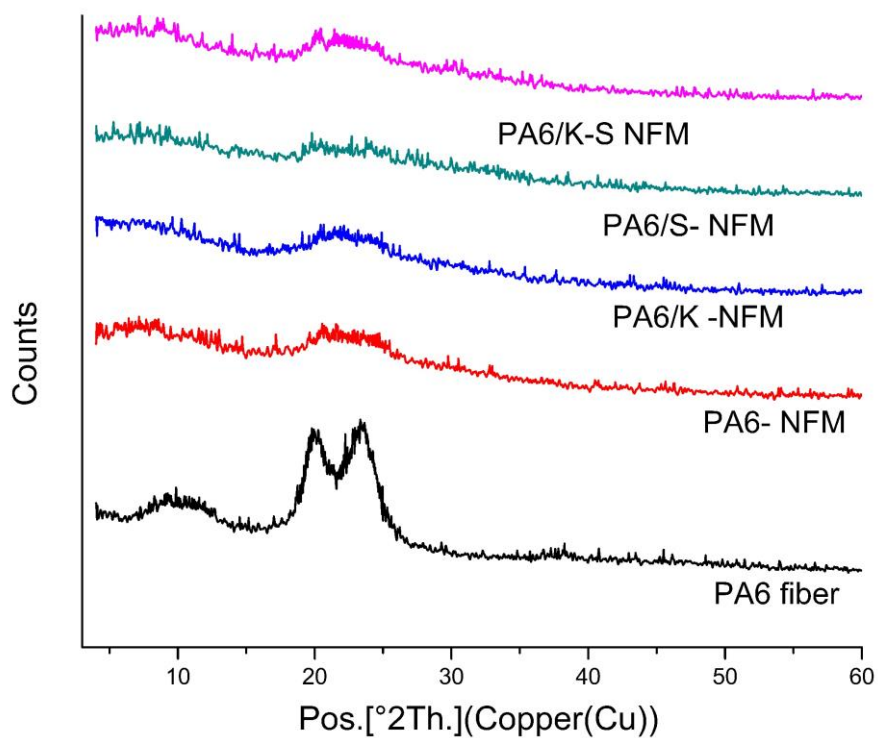| Sample	2θ	d-spacing (Å)	Crystallinity index (%)
PA6 fibers	20.2	4.4	43. 0
	23.4	3.8	
Keratin powder	19.8	4.5	38. 0
	10.0	8.8	
Sericin powder	14.6	6.1	39.7
	11.7	7.5	
PA6-NFM	21.8	4.1	33. 0
	23.9	3.7	
PA6/S NFM	24.1	3.7	40.9
	9.1	9.5	
PA6/K NFM	21.9	4.1	59.0
	6.8	13.1	
PA6/K-S NFM	20.3	4.4	47.5
	6.7	13.2	

Figure 6. XRD pattern of PA6 fiber, PA6-NFM,
PA6/K, PA6/S and PA6/K-S NFMs.

4. Conclusions

PA 6-based NFMs with sericin and keratin wastes were successfully electro-spun into NFM. The prepared mats have the potential for sorption of heavy metal cations as well as the anionic and cationic dyes from wastewater for different extents depending on the composition of the NFM and the nature of the dye or cation; the exposure time is also another important concern. The efficiency of all examined NFMs for adsorption of cations from their solution is in the order: $Cr^{+6}>Pb^{+2}>Cr^{+3}>Cu^{+2}$. The efficiency of the used NFMs in sorption of Cr^{+6} and Pb^{+2} ions from their aqueous solutions was found to be PA6/S ≈ PA6/K-S > PA6/K > PA6 and PA6/K > PA6 > PA6/K/S > PA6/S, respectively. The results of XRD, TGA, and DSC assure that keratin and sericin reinforced PA 6 NFMs have higher crystallinity, and thermal stability than the corresponding native polymers.

This work has positive environmental and economic impact by virtue of the extraction of keratin and sericin from waste materials followed by their utilization in reinforcement and functionalization of PA6 nanofibrous mats for sorption of heavy metal ions as well as dyes from textile effluents. Further work will be conducted in our laboratory for analysis of the surface properties of the prepared NFMs using some techniques such as AFM and XPS.

Acknowledgments

References

Abdel–Gawad, S. A., & Abd El–Aziz, H. M. (2019). Removal of pharmaceuticals from aqueous medium using entrapped activated carbon in alginate. *Air, Soil and Water Research*, 12, 1-7. https://doi.org/10.1177/1178622119848761

Abdel-Halim, S. H., Shehata, A. M. A., & El-Shahat, M. F. (2003). Removal of lead ions from industrial waste water by different types of natural materials. *Water Research, 37*(7), 1678-1683. https://doi.org/10.1016/S0043-1354(02)00554-7

Abou Taleb, M., Mowafi, S., & El-Sayed, H. (2020). Utilization of keratin or sericin-based composite in detection of free chlorine in water. *Journal of Molecular Structure*, 1202, 127379. https://doi.org/10.1016/j.molstruc.2019.127379

Abou Taleb, M., Mowafi, S., El-Sayed, H., & El-Newashy, R. (2019). Facile development of electrically conductive comfortable fabrics using metal ions. *Journal of Industrial Textiles*. https://doi.org/10.1177%2F1528083719893713

Aizawa, T., & Wakui, Y. (2020). Correlation between the Porosity and Permeability of a Polymer Filter Fabricated via CO$_2$-Assisted Polymer Compression. *Membranes, 10*(12), 391. https://doi.org/10.3390/membranes10120391

Alhujaily, A., Yu, H., Zhang, X., & Ma, F. (2020). Adsorptive removal of anionic dyes from aqueous solutions using spent mushroom waste. *Applied Water Science, 10*(7), 1-12. https://doi.org/10.1007/s13201-020-01268-2

Al-Shannag, M., Al-Qodah, Z., Bani-Melhem, K., Qtaishat, M. R., & Alkasrawi, M. (2015). Heavy metal ions removal from metal plating wastewater using electrocoagulation: Kinetic study and process performance. *Chemical Engineering Journal, 260*, 749-756. https://doi.org/10.1016/j.cej.2014.09.035

Aneyo, I. A., Doherty, F. V., Adebesin, O. A., & Hammed, M. O. (2016). Biodegradation of pollutants in waste water from pharmaceutical, textile and local dye effluent in lagos, Nigeria. *Journal of Health and Pollution, 6*(12), 34-42. https://doi.org/10.5696/2156-9614-6.12.34

Awual, M. R. (2015). A novel facial composite adsorbent for enhanced copper (II) detection and removal from wastewater. *Chemical Engineering Journal, 266*, 368-375. https://doi.org/10.1016/j.cej.2014.12.094

Balamurugan, R., Sundarrajan, S., & Ramakrishna, S. (2011). Recent trends in nanofibrous membranes and their suitability for air and water filtrations. *Membranes, 1*(3), 232-248. https://doi.org/10.3390/membranes1030232

Bohli, T., Ouederni, A., Fiol, N., & Villaescusa, I. (2015). Evaluation of an activated carbon from olive stones used as an adsorbent for heavy metal removal from aqueous phases. *Comptes rendus chimie, 18*(1), 88-99. https://doi.org/10.1016/j.crci.2014.05.009

Carus, M., Baltus, W., Carrez, D., Kaeb, H., Ravenstijn, J., & Zepnik, S. (2013). Market study and database on bio-based polymers in the world. *Nova-Institute GmbH: Huerth, 7*(1).

Chakraborty, J. N. (Ed.). (2015). Fundamentals and practices in colouration of textiles. CRC Press.

Chen, S. S., Hsu, B. C., Ko, C. H., & Chuang, P. C. (2008). Recovery of chromate from spent plating solutions by two-stage nanofiltration processes. *Desalination, 229*(1-3), 147-155. https://doi.org/10.1016/j.desal.2007.08.015

Cheng, X. W., Guan, J. P., Chen, G., Yang, X. H., & Tang, R. C. (2016). Adsorption and flame retardant properties of bio-based phytic acid on wool fabric. *Polymers, 8*(4), 122. https://doi.org/10.3390/polym8040122

Dhineshbabu, N. R., Manivasakan, P., & Rajendran, V. (2014). Hydrophobic and thermal behaviour of nylon 6 nanofibre web deposited on cotton fabric through electrospinning. *Micro & Nano Letters, 9*(8), 519-522. https://doi.org/10.1049/mnl.2014.0161

El-Gabry, L., Abou El-Kheir, A., Salama, M., Mowafi, S., & El-Sayed, H. (2016). Acrylic/keratin composite of enhanced dyeability towards cationic and anionic dyes. *Coloration Technology, 132*(1), 83-91. https://doi.org/10.1111/cote.12190

El-Newashy, R. F., Mowafi, S., Haggag, K., Abou Taleb, M., & El-Sayed, H. (2019). Evaluation of Comfort Attributes of Polyester Knitted Fabrics Treated with Sericin. *Fibers and Polymers, 20*(9), 1992-2001. https://doi.org/10.1007/s12221-019-9275-3

El-Sayed, H. (2006). Novel approach for antisetting of wool fabrics during dyeing. *Coloration technology, 122*(1), 57-60. https://doi.org/10.1111/j.1478-4408.2006.00004.x

El-Sayed, H., Kantouch, A., & Raslan, W. M. (2004). Environmental and technological studies on the interaction of wool with some metal ions. *Toxicological & Environmental Chemistry, 86*(3), 141-146. https://doi.org/10.1080/02772240410001688233

El-Sayed, H., Vineis, C., Varesano, A., Mowafi, S., Carletto, R. A., Tonetti, C., & Abou Taleb, M. (2019). A critique on multi-jet electrospinning: State of the art and future outlook. *Nanotechnology Reviews, 8*(1), 236-245.

El-Sherif, I. Y., Tolani, S., Ofosu, K., Mohamed, O. A., & Wanekaya, A. K. (2013). Polymeric nanofibers for the removal of Cr (III) from tannery waste water. *Journal of environmental management, 129*, 410-413. https://doi.org/10.1016/j.jenvman.2013.08.004

Fornes, T. D., & Paul, D. R. (2003). Crystallization behavior of nylon 6 nanocomposites. *Polymer, 44*(14), 3945-3961. https://doi.org/10.1016/S0032-3861(03)00344-6

Gautam, R. K., Gautam, P. K., Banerjee, S., Soni, S., Singh, S. K., & Chattopadhyaya, M. C. (2015). Removal of Ni (II) by magnetic nanoparticles. *Journal of molecular liquids, 204*, 60-69. https://doi.org/10.1016/j.molliq.2015.01.038

Goel, J., Kadirvelu, K., Rajagopal, C., & Garg, V. K. (2005). Removal of lead (II) by adsorption using treated granular activated carbon: batch and column studies. *Journal of hazardous materials, 125*(1-3), 211-220. https://doi.org/10.1016/j.jhazmat.2005.05.032

Gopal, R., Kaur, S., Feng, C. Y., Chan, C., Ramakrishna, S., Tabe, S., & Matsuura, T. (2007). Electrospun nanofibrous polysulfone membranes as pre-filters: Particulate removal. *Journal of membrane science, 289*(1-2), 210-219. https://doi.org/10.1016/j.memsci.2006.11.056

Gopal, R., Kaur, S., Ma, Z., Chan, C., Ramakrishna, S., & Matsuura, T. (2006). Electrospun nanofibrous filtration membrane. *Journal of Membrane Science, 281*(1-2), 581-586. https://doi.org/10.1016/j.memsci.2006.04.026

Gu, S., Kang, X., Wang, L., Lichtfouse, E., & Wang, C. (2019). Clay mineral adsorbents for heavy metal removal from wastewater: a review. *Environmental Chemistry Letters, 17*(2), 629-654. https://doi.org/10.1007/s10311-018-0813-9

Haeri, M., & Haeri, M. (2015). ImageJ plugin for analysis of porous scaffolds used in tissue engineering. *Journal of Open Research Software, 3*(1). http://doi.org/10.5334/jors.bn

Haggag, K., Kantouch, F., Allam, O. G., & El-Sayed, H. (2009). Improving Printability of Wool Fabrics Using Sericin. *Journal of Natural Fibers, 6*(3), 236-247. https://doi.org/10.1080/15440470902975292

Haider, A., Haider, S., & Kang, I. K. (2018). A comprehensive review summarizing the effect of electrospinning parameters and potential applications of nanofibers in biomedical and biotechnology. *Arabian Journal of Chemistry, 11*(8), 1165-1188. https://doi.org/10.1016/j.arabjc.2015.11.015

He, X., Cheng, L., Wang, Y., Zhao, J., Zhang, W., & Lu, C. (2014). Aerogels from quaternary ammonium-functionalized cellulose nanofibers for rapid removal of Cr (VI) from water. *Carbohydrate polymers, 111*, 683-687. https://doi.org/10.1016/j.carbpol.2014.05.020

Hua, M., Zhang, S., Pan, B., Zhang, W., Lv, L., & Zhang, Q. (2012). Heavy metal removal from water/wastewater by nanosized metal oxides: a review. *Journal of hazardous materials, 211*, 317-331. https://doi.org/10.1016/j.jhazmat.2011.10.016

Jose, S., Shanmugam, N., Das, S., Kumar, A., & Pandit, P. (2019). Coating of lightweight wool fabric with nano clay for fire retardancy. *The Journal of the Textile Institute, 110*(5), 764-770. https://doi.org/10.1080/00405000.2018.1516529

Kannan, N., & Sundaram, M. M. (2001). Kinetics and mechanism of removal of methylene blue by adsorption on various carbons—a comparative study. *Dyes and pigments, 51*(1), 25-40. https://doi.org/10.1016/S0143-7208(01)00056-0

Kantouch, A., Khalil, E. M., Mowafi, S., Allam, O. G., & El-Sayed, H. (2011). Utilization of ionic liquids for low temperature dyeing of proteinic fabrics. *Egyptian Journal of Chemistry, 54*(2), 189-203. https://doi.org/10.21608/ejchem.2011.1388

Kantouch, A., Allam, O., El-Gabry, L., & El-Sayed, H. (2012). Effect of pretreatment of wool fabric with keratin on its dyeability with acid and reactive dyes. *Indian. Journal Fiber Textile Research 37*, 157–161.

Karthik, R., & Meenakshi, S. (2015). Removal of Pb (II) and Cd (II) ions from aqueous solution using polyaniline grafted chitosan. *Chemical Engineering Journal, 263*, 168-177. https://doi.org/10.1016/j.cej.2014.11.015

Liu, D., Zhu, Y., Li, Z., Tian, D., Chen, L., & Chen, P. (2013). Chitin nanofibrils for rapid and efficient removal of metal ions from water system. *Carbohydrate polymers, 98*(1), 483-489. https://doi.org/10.1016/j.carbpol.2013.06.015

Liu, Y., Yu, X., Li, J., Fan, J., Wang, M., Lei, T. D., ... & Huang, D. (2015). Fabrication and properties of high-content keratin/poly (ethylene oxide) blend nanofibers using two-step cross-linking process. *Journal of Nanomaterials*, 2015. https://doi.org/10.1155/2015/803937

Lunge, S., Singh, S., & Sinha, A. (2014). Magnetic iron oxide (Fe_3O_4) nanoparticles from tea waste for arsenic removal. *Journal of Magnetism and Magnetic Materials, 356*, 21-31. https://doi.org/10.1016/j.jmmm.2013.12.008

Madadrang, C. J., Kim, H. Y., Gao, G., Wang, N., Zhu, J., Feng, H., ... & Hou, S. (2012). Adsorption behavior of EDTA-graphene oxide for Pb (II) removal. *ACS applied materials & interfaces, 4*(3), 1186-1193. https://doi.org/10.1021/am201645g

Mahapatra, A., Mishra, B. G., & Hota, G. (2013). Electrospun Fe_2O_3–Al_2O_3 nanocomposite fibers as efficient adsorbent for removal of heavy metal ions from aqueous solution. *Journal of hazardous Materials, 258*, 116-123. https://doi.org/10.1016/j.jhazmat.2013.04.045

Mnif, A., Bejaoui, I., Mouelhi, M., & Hamrouni, B. (2017). Hexavalent chromium removal from model water and car shock absorber factory effluent by nanofiltration and reverse osmosis membrane. *International journal of analytical chemistry*, 2017. https://doi.org/10.1155/2017/7415708

Mit-uppatham, C., Nithitanakul, M., & Supaphol, P. (2004). Ultrafine electrospun polyamide-6 fibers: effect of solution conditions on morphology and average fiber diameter. *Macromolecular Chemistry and Physics, 205*(17), 2327-2338. https://doi.org/10.1002/macp.200400225

Mobasherpour, I., Salahi, E., & Pazouki, M. (2012). Comparative of the removal of Pb^{2+}, Cd^{2+} and Ni^{2+} by nano crystallite hydroxyapatite from aqueous solutions: Adsorption isotherm study. *Arabian Journal of Chemistry, 5*(4), 439-446. https://doi.org/10.1016/j.arabjc.2010.12.022

Moore, C. J. (2008). Synthetic polymers in the marine environment: a rapidly increasing, long-term threat. *Environmental research, 108*(2), 131-139. https://doi.org/10.1016/j.envres.2008.07.025

Mowafi, S., Abou Taleb, M., & El-Sayed, H. (2018). Towards analytical stripes for detection of iron III cations in domestic water using proteinic biopolymers. *Journal of Cleaner Production, 202, 45-53.* https://doi.org/10.1016/j.jclepro.2018.08.141

Nabeela Nasreen, S. A. A., Sundarrajan, S., Syed Nizar, S. A., & Ramakrishna, S. (2019). Nanomaterials: solutions to water-concomitant challenges. *Membranes, 9*(3), 40. https://doi.org/10.3390/membranes9030040

Nezarati, R., Eifert, M. and Cosgriff-Henandez, E, (2013), Effects of humidity and solution viscosity of electrospunfibremosphology, *Tissue Eng Part C Methods. 19*, 810–819. https://doi.10.1089/ten.TEC.2012.0671

Pohl, A. (2020). Removal of Heavy Metal Ions from Water and Wastewaters by Sulfur-Containing Precipitation Agents. *Water Air Soil Pollut, 231*, 503.
https://doi.org/10.1007/s11270-020-04863-w

Rad, L. R., Momeni, A., Ghazani, B. F., Irani, M., Mahmoudi, M., & Noghreh, B. (2014). Removal of Ni^{2+} and Cd^{2+} ions from aqueous solutions using electrospun PVA/zeolite nanofibrous adsorbent. *Chemical Engineering Journal, 256*, 119-127.
https://doi.org/10.1016/j.cej.2014.06.066

Ki, C. S., Kim, J. W., Oh, H. J., Lee, K. H., & Park, Y. H. (2007). The effect of residual silk sericin on the structure and mechanical property of regenerated silk filament. International *Journal of Biological Macromolecules, 41*(3), 346-353.
https://doi.org/10.1016/j.ijbiomac.2007.05.005

Sounthararajah, D. P., Loganathan, P., Kandasamy, J., & Vigneswaran, S. (2015). Adsorptive removal of heavy metals from water using sodium titanate nanofibres loaded onto GAC in fixed-bed columns. *Journal of hazardous materials, 287*, 306-316.
https://doi.org/10.1016/j.jhazmat.2015.01.067

Sum, J. Y., Ahmad, A. L., & Ooi, B. S. (2019). Selective separation of heavy metal ions using amine-rich polyamide TFC membrane. *Journal of Industrial and Engineering Chemistry, 76*, 277-287.
https://doi.org/10.1016/j.jiec.2019.03.052

Tetteh, E. K., & Rathilal, S. (2021). Application of magnetized nanomaterial for textile effluent remediation using response surface methodology. *Materials Today: Proceedings, 38*, 700-711.
https://doi.org/10.1016/j.matpr.2020.03.827

Tsai, P. P., Schreuder-Gibson, H., & Gibson, P. (2002). Different electrostatic methods for making electret filters. *Journal of electrostatics, 54*(3-4), 333-341.
https://doi.org/10.1016/S0304-3886(01)00160-7

Ucun, H., Bayhana, Y. K., Kaya, Y., Cakici, A., & Algur, O. F. (2003). Biosorption of lead (II) from aqueous solution by cone biomass of *Pinus sylvestris*. *Desalination, 154*(3), 233-238.
https://doi.org/10.1016/S0011-9164(03)80038-3

Vitchuli, N., Shi, Q., Nowak, J., Kay, K., Caldwell, J. M., Breidt, F., ... & Zhang, X. (2011). Multifunctional ZnO/Nylon 6 nanofiber mats by an electrospinning–electros praying hybrid process for use in protective applications. *Science and technology of advanced materials.*
https://doi.org/10.1088/1468-6996/12/5/055004

Wang, J., Xu, W., Chen, L., Huang, X., & Liu, J. (2014). Preparation and evaluation of magnetic nanoparticles impregnated chitosan beads for arsenic removal from water. *Chemical Engineering Journal, 251*, 25-34.
https://doi.org/10.1016/j.cej.2014.04.061

Xu, J., Zhang, H., Zhang, J., & Kim, E. J. (2014). Capture of toxic radioactive and heavy metal ions from water by using titanate nanofibers. *Journal of alloys and compounds, 614*, 389-393.
https://doi.org/10.1016/j.jallcom.2014.06.128

Xu, M., Hadi, P., Chen, G., & McKay, G. (2014). Removal of cadmium ions from wastewater using innovative electronic waste-derived material. *Journal of Hazardous Materials, 273*, 118-123.
https://doi.org/10.1016/j.jhazmat.2014.03.037

Zhao, R., Li, X., Sun, B., Shen, M., Tan, X., Ding, Y., ... & Wang, C. (2015). Preparation of phosphorylated polyacrylonitrile-based nanofiber mat and its application for heavy metal ion removal. *Chemical Engineering Journal, 268*, 290-299.
https://doi.org/10.1016/j.cej.2015.01.061

Zoccola, M., Montarsolo, A., Aluigi, A., Varesano, A., Vineis, C., & Tonin, C. (2007). Electrospinning of polyamide 6/modified-keratin blends. *e-Polymers, 7*(1).
https://doi.org/10.1515/epoly.2007.7.1.1204

Zhang, X., & Wyeth, P. (2010). Using FTIR spectroscopy to detect sericin on historic silk. *Science China Chemistry, 53*(3), 626-631.
https://doi.org/10.1007/s11426-010-0050-y

Zhou, W., He, J., Cui, S., & Gao, W. (2011). Preparation of electrospun silk fibroin/Cellulose Acetate blend nanofibers and their applications to heavy metal ions adsorption. Fibers and Polymers, 12(4), 431-437.
https://doi.org/10.1007/s12221-011-0431-7